



RESEARCH ARTICLE

A study on safe navigation towards intelligent shipping considering sea conditions

Gökhan Budak^{1*}

¹ İzmir Katip Çelebi University, Faculty of Naval Architecture and Maritime, Department of Shipbuilding and Ocean Engineering, İzmir, Türkiye

ARTICLE INFO

Article History:
Received: 06.08.2023
Received in revised form: 25.08.2023
Accepted: 27.08.2023
Available online: 28.09.2023

Keywords:
Ship maneuvering
Safe navigation
Regular head waves
Path following

ABSTRACT

A mathematical model is created to obtain safe navigation for ships in regular head waves in this study. To validate the suggested model, firstly, the added resistances are calculated for two different ships using empirical formulas in the mathematical model. Secondly, the turning test simulations are performed for calm water and in waves with various wave amplitudes. After these validation studies, the path following simulation of the ship to the target destinations is performed in both waves and calm water for the determined course. It is assumed that regular head waves affect the ship as an external disturbance. The wavelengths and wave amplitudes are changed systematically to understand their effect during the path following simulations. When the ratio of wavelength to ship length, λ/L_{pp} , is nearly 1.0, the path following simulation times increase. Moreover, when the value of wave amplitude increases, so does the simulation time.

Please cite this paper as follows:

Budak, G. (2023). A study on safe navigation towards intelligent shipping considering sea conditions. *Marine Science and Technology Bulletin*, 12(3), 370-379. <https://doi.org/10.33714/masteb.1338476>

Introduction

Automatic control systems have been seen frequently in all fields of science. Nowadays, road and rail vehicles have been equipped with autonomous systems in all aspects, thanks to the technological developments. Moreover, there is a remarkable interest in autonomous shipping due to positive feedbacks obtained from applications in train and car industries. In this context, the similar expectations for autonomous ships reveal with the promises of autonomous applications in shipping to

provide operational, economic, and ecological sustainability. The main promise of autonomous ships is safe navigation for all components in shipping. For example, human decisions can be risky since there are too many variables in some situations such as collision risk and bad weather condition. However, it can be safer when a critical decision given by the onboard intelligent systems analyzing all changing parameters. On the other hand, these systems are important not only for safe navigation, but also for economic and sustainable operations (Akbar et al., 2021; Kurt & Aymelek, 2022; Kafalı & Aksu,

* Corresponding author

E-mail address: gokhan.budak@ikc.edu.tr (G. Budak)



2022). Although it is thought that the transition to autonomous shipping is its infant age, there is an opportunity to operate ships under control with autonomous systems thanks to obtained positive outputs from sea trials. This study proposes a mathematical model including a basic intelligent control system to ensure safe navigation in regular head wave by avoiding possible collision risk.

The previous studies in the literature aimed to safely finish the ship's movement considering environmental conditions, reducing fuel consumption, or shortening the ship's berthing time at the port. The intelligent controller systems, such as PID (Proportional Integral Derivative), fuzzy logic, and neural networks etc., are commonly performed by researchers to achieve these goals. Safe navigation on a created course is one of the main aims of the previous studies in the literature. For instance, Moreira et al. (2007) proposed a control system for path following application based on LOS (light of sight) guidance. In their research, the proposed system was verified for the Esso Osaka and the simulations were performed for different desired geometrical paths. In another study, Zaccone & Martelli (2020) studied on a collision avoidance system based on Rapidly Exploring Random Tree (RRT*) algorithm for surface vessel navigation. Additionally, Mohamed-Seghir et al. (2021) developed an intelligent system based on fuzzy logic to determine a ship route in the event of the collision risks and reduce energy consumption. In a similar study, Chen et al. (2021) investigated a smart control system based on fuzzy sets for unmanned surface vessel to avoid the collision. This investigation applied both the fixed obstacles and incoming ships' encounter situations. Zhou et al. (2021) used the traditional PID as a control system for collision avoidance and path following simulations. Moreover, there are studies in the literature including more than one control system among the proposed methods for both path following and collision avoidance. For example, He et al. (2021) used not only fuzzy but also PID controller to determine the optimal route to avoid the collision. The different mathematical models to avoid the collision are proposed by the researchers (Degre & Lefevre, 1981; Fossen, 2002). Many control systems based on various algorithms can be found in the literature. Tsou & Hsueh (2010) proposed a mathematical model including avoidance collision system based on Art Colony Optimization Algorithm. Lyu & Yin (2017) introduced a trajectory planning algorithm modified artificial potential field to navigate safely. Perera et al. (2010) presented a collision-avoidance system that used a Bayesian Network decision-making process to avoid collision with multiple ships. The algorithm based on neural network is

one of them which is applied on collision avoidance simulations (Praczyk, 2015; Wang & Fu, 2020; Suo et al., 2020). Other worth-to-mention proposed algorithms to solve the same problem were explained in the studies (Liu et al., 2020; Zhao et al., 2021). All these mentioned mathematical models, including different control algorithms and/or numerical approaches, show that safe navigation is an interesting topic for researchers.

The forces and moments that the ship will be exposed to due to external disturbances will also affect the movements of the ship. For instance, the studies that analyze the calculation of wave-induced forces and moments as well as how these forces and moments affect ships are extremely popular. Among these studies, Beji (2020) formulated the waves and currents forces acting on a body. Xie et al. (2020) numerically calculated the turning circle tests under the effect of waves with varying wavelengths for two different ships. Similarly, Fang et al. (2005) simulated the turning test of a ship under the effect of waves. In another study, Jin et al. (2021) performed turning circle test simulations with the URANS (Unsteady Reynolds-Averaged Navier-Stokes) equations based on CFD (Computational Fluid Dynamics). In another study, the added resistance of a model ship with the constant forward velocity in waves was calculated using URANS equations (Ozdemir & Barlas, 2017). Furthermore, Park et al. (2016) studied on added resistance induced head waves for different draft value of ship. The effects of external disturbances such as current and wind, as well as wave-induced forces, have been studied in the literature (Szelangiewicz et al., 2014; Yasukawa & Sakuno, 2019). Besides these studies, a comprehensive review including studies of investigating the effects of external disturbances on ship motions and maneuvering was presented by Hirdaris et al. (2014).

In this study, the control system, which is one of the intelligent transportation systems that should be on an autonomous ship, has been added to the mathematical model. Thus, the ship can reach the target area by avoiding collision in regular head waves thanks to this control system. To validate the proposed mathematical model, firstly, the added resistances are calculated for the KVLCC2 ship to validate the regular wave forces, and then these results are compared with the other studies in the literature. Secondly, the turning circle test simulations for the Esso Osaka ship having limited studies comparison to the KVLCC2 ship are performed in regular head waves having different wave amplitudes. Finally, a random course with fixed obstacles is determined for the Esso Osaka to perform the simulations. These simulations are carried out both in regular head waves and calm water to understand the effects

of the waves using the mathematical model. Moreover, it is discussed whether the ship could reach the target coordinates and create a safe route automatically to avoid collisions on the determined course.

Material and Method

Maneuvering Model

The MMG (Maneuvering Modeling Group) model was added to the literature by Ogawa & Kasai (1978). In this maneuvering model, the forces and the moment acting on a ship are calculated separately based on the hull, propeller, rudder, and external forces. The MMG model is widely preferred to obtain information about ship maneuvering (Yasukawa & Yoshimura, 2015; Aksu & Köse, 2017). In this study, regular head wave is assumed as an external force.

The mathematical model is created based on the MMG model to calculate all these forces and moments. The equations for surge, sway and yaw motions may be written in Eq. 1.

$$\begin{aligned}
 (m + m_x)\dot{u} - (m + m_y)vr - mx_G r^2 &= X \\
 (m + m_y)\dot{v} + (m + m_x)ur + mx_G \dot{r} &= Y \\
 (I_{zz} + mx_G^2 + J_{zz})\dot{r} + mx_G(\dot{v} + ur) &= N
 \end{aligned}
 \tag{1}$$

where m , ship mass; m_x and m_y , the added masses; I_{zz} the mass moment of inertia; J_{zz} , the added mass moment of inertia; u and v the velocity components of ship velocity; r , angular velocity of ship, and x_G the distance between origin and the gravity center of the ship.

The fixed and moving coordinates of ship are described for the mathematical model and other relevant quantities are shown in Figure 1.

The total forces and moment can be expressed as the sum of the hull, propeller, rudder, and wave forces and moment for this study.

The hydrodynamic forces and moment for ship hull are calculated with Eq. 2.

$$\begin{aligned}
 X_H &= -R_0 + X_{vv}v^2 + X_{vr}vr + X_{rr}r^2 + X_{vvv}v^4 \\
 Y_H &= Y_vv + Y_r r + Y_{vvv}v^3 + Y_{vvr}v^2r + Y_{vrr}vr^2 + Y_{rrr}r^3 \\
 N_H &= N_vv + N_r r + N_{vvv}v^3 + N_{vvr}v^2r + N_{vrr}vr^2 + N_{rrr}r^3
 \end{aligned}
 \tag{2}$$

While calculating the propeller-induced force on x-direction, Eq. 3 may be written depending on thrust deduction

factor (t) and propeller thrust (T). The force on y-direction Y_P and the moment N_P are accepted as zero.

$$X_P = (1 - t)T \tag{3}$$

Eq. 4 expresses rudder-induced forces and moment. The forces and moment depending on the changing rudder angle can be calculated using this equation. The expression of the rudder normal force is $F_N = (1/2)\rho A_R U_R^2 f_\alpha \sin\alpha_R$.

$$\begin{aligned}
 X_R &= -(1 - t_R)F_N \sin\delta \\
 Y_R &= -(1 - a_H)F_N \cos\delta \\
 N_R &= -(x_R + a_H x_H)F_N \cos\delta
 \end{aligned}
 \tag{4}$$

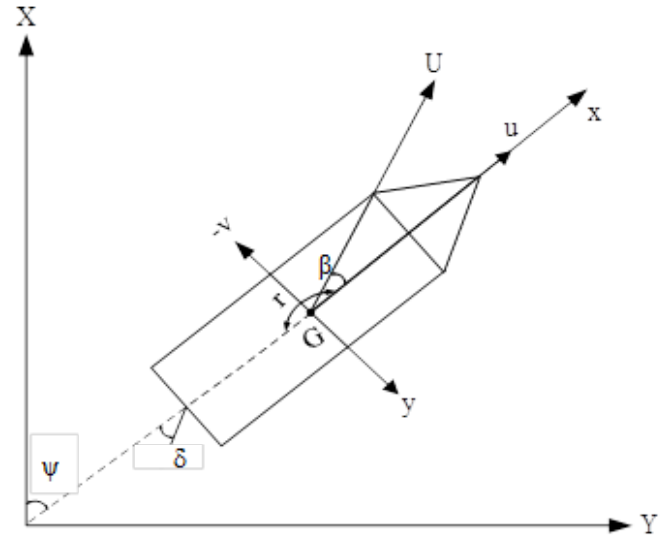


Figure 1. Fixed and ship coordinates

The added resistance values can be obtained by using experimental methods (Lee et al., 2013) numerical calculations (Sadat-Hosseini et al., 2013; Çakıcı et al., 2017), and empirical formulas. Since the fastest one among them is the empirical formulas, it is implemented for this study. The empirical formulas to calculate the total added resistance due to the regular head waves given in Eq. 5 is chosen from the studies in the literature. More details information about these empirical formulas can be seen in the studies of (Tsujiimoto et al., 2008; Liu & Papanikolaou, 2016; Liu et al., 2020; Lang & Mao, 2020).

$$R_{AW} = R_{AWR} + R_{AWM} \tag{5}$$

The first part of the total added resistance (R_{AWR}) will be calculated using Eq. 6, and Eq. 7 may be used to calculate the second part of the total resistance (R_{AWM}).

$$R_{AWR} = \frac{2.25}{2} \rho g \zeta_a^2 \alpha_T \sin^2 E \left(1 + 5 \sqrt{\frac{L_{pp}}{\lambda}} Fn \right) \left(\frac{0.87}{C_B} \right)^{1+4\sqrt{Fn}} \quad (6)$$

where ρ , is the density; g , gravity acceleration; ζ_a , the incident wave amplitude; L_{pp} , length between perpendiculars; λ , the wavelength; Fn , Froude number; C_B , block coefficient; $E = \text{atan} \left(\frac{B}{2L_E} \right)$, waterline entrance angle; L_E waterline entrance length.

$$R_{AWM} = 4 \rho g \zeta_a^2 \frac{B^2}{L_{pp}} \bar{\omega}^{b_1} \exp \left[\frac{b_1}{d_1} (1 - \bar{\omega}^{d_1}) \right] a_1 a_2 a_3 \quad (7)$$

where the parameters $\bar{\omega}$, b_1 , d_1 , a_1 , a_2 , a_3 can be calculated using empirical formulas are given by Liu & Papanikolaou (2017).

The dimensionless wave induced force and moment can be calculated using Eq. 8 (Li & Zhang, 2022). The dimensionless force coefficient Y_W' is multiplied by $(1/2)\rho L^2 U^2$ to make dimensional. Similarly, the dimensionless moment coefficient N_W' is multiplied by $(1/2)\rho L^3 U^2$.

$$Y_W' = -2aL \frac{\sin(b) \sin(c)}{b} s(t)$$

$$N_W' = ak \left(B^2 \sin(b) \frac{c \cos(c) - \sin(c)}{c^2} - L^2 \sin(c) \frac{b \cos(b) - \sin(b)}{b^2} \right) \xi(t) \quad (8)$$

where the parameters can be express as $a = \rho g (1 - e^{kT}) / k^2$, $b = (kL \cos(\chi)) / 2$, $c = (kB \sin(\chi)) / 2$, $k = \frac{2\pi}{\lambda}$, χ is the wave direction.

Controller

In the simulated application, the classical PD controller given Eq. 9 and proposed algorithm are used as the control system to obtain the ship route and to avoid collision. The controller gains, K_p and K_d , have been determined with Matlab-PID Tuner. When the ship encounters any obstacle while following the determined course, Eq. 11 and Eq. 12 are used, otherwise Eq. 10 is used to calculate the desired ship heading angle.

$$\delta(t) = K_p e(t) + K_d \frac{de(t)}{dt} \quad (9)$$

where $\delta(t)$, the rudder angle; $e(t)$, the error.

The calculation of the ship's heading angle differs depending on whether there is an obstacle between any two points on the determined course. If there is no obstacle between the determined coordinates on the course, the desired ship heading angle ψ_d is calculated for the target coordinates. The

ship has been no sooner arrived the target coordinates than the desired heading angle has been calculated automatically for the next target coordinates. The changing of desired ship heading depends on the coordinates of ship (x_{sp}, y_{sp}) and the destination point (x_{dp}, y_{dp}) .

$$\psi_d = \text{atan} \left(\frac{y_{dp} - y_{sp}}{x_{dp} - x_{sp}} \right) \quad (10)$$

If there is an obstacle on the course, the ship will maneuver to avoid the collision risk. To avoid the collision, the obstacle coordinates and the maximum length of obstacle should be entered into the mathematical model as data, initially. The safe coordinates are determined thanks to the mathematical model according to the size and distance of the obstacle. The required heading angle to reach the target virtual coordinates is accepted as the reference angle for each virtual coordinate and the needed angle is commanded to the rudder. The ship continues to follow the course thanks to the controller system since the commanded rudder angle for the next target coordinates on the course has been changed. The following chart given in Figure 2 explains safe navigation in the mathematical model according to the position of the obstacles.

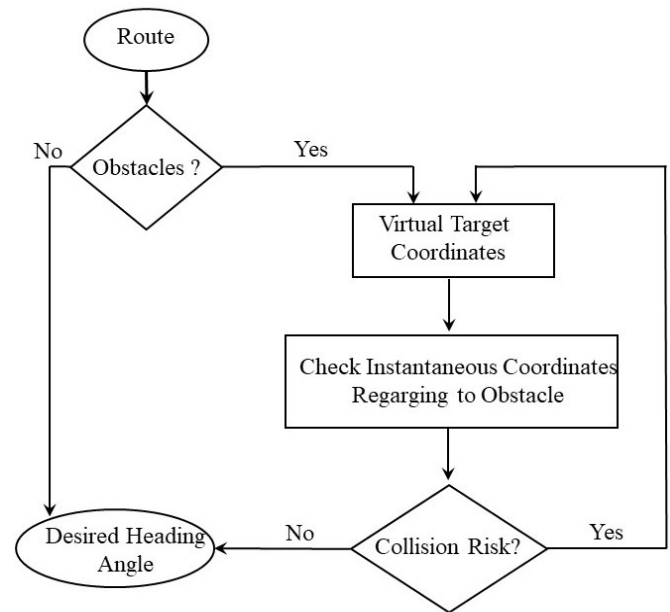


Figure 2. Flow diagram

If the ship encounters an obstacle on the determined course, the ship may follow the route without collision by assistance of the virtual target coordinates. Meanwhile, these virtual coordinates are used to obtain a safe route.

$$SY_{pe1} = Y_{obs} - y_{sp}$$

$$SX_{pe1} = X_{obs} - x_{sp}$$

$$S\psi_{pe1} = \text{atan}\left(\frac{SY_{pe1}}{SX_{pe1}}\right) \quad (11)$$

where X_{obs} , Y_{obs} are the coordinates of the obstacle.

$$SY_{pe2} = Y_{obs} + D + D * \cos\left(\left(\frac{\pi}{2}\right) - S\psi_{pe1}\right)$$

$$SX_{pe2} = X_{obs} + D * \sin(S\psi_{pe1})$$

$$S\psi_{pe2} = \text{atan}\left(\frac{SY_{pe2}}{SX_{pe2}}\right) \quad (12)$$

D is value of the maximum safe zone length. The maneuvering characteristics are the remarkable parameters to determine the virtual coordinates 1 since the ship has enough length to maneuver before the safe zone. The part of the algorithm for avoiding the collision is shown in Eq. 11 and Eq. 12. Briefly, the virtual coordinates 1, SX_{pe1} and SY_{pe1} , the difference between the coordinates of obstacles, and the ship, are calculated at each time step until a certain distance obtained from the safe zone calculated for the ship's maneuvering ability. When the ship reaches virtual coordinates 1; the ship maneuver to the virtual coordinates 2, given in Eq. 12, to avoid the collision. When the ship reaches virtual coordinates 2, the rudder angle is changed for the target coordinates. Other detailed information can be seen in Budak (2023).

Results and Discussion

Simulation Study

In the scope of this study, three different simulations are performed using the mathematical model. Firstly, the added resistances depending on various wavelength are calculated for KVLCC2 at $Fn=0.142$ for validation purpose. Since the lack of experimental data or numerical calculations for Esso Osaka ship in regular head wave, the simulation results are only compared with numerical calculations for KVLCC2. Secondly, after validating the mathematical model for regular head wave, the simulations are enlarged for turning tests of the Esso Osaka ship. These turning test simulations are performed for different wave amplitudes and the obtained results for turning trajectories of the Esso Osaka ship are evaluated under same wavelength ($\lambda/L_{pp}=1.0$) of regular head waves. Lastly, the path following simulations are carried out for determined course in regular head waves.

The basic dimensions, seen in Table 1, and the required maneuvering derivatives in MMG model for these ships can be

seen in the studies of (Kobayashi et al., 2002; Abdel-latif et al., 2013; Yasukawa & Yoshimura, 2015).

Table 1. Main sizes of the ships

	KVLCC2	Esso Osaka
L_{pp} (m)	320	325
B (m)	58	53
T (m)	20.8	22.05
C_B (-)	0.81	0.831
U (knot)	15.5	10

Validation Study

The added resistance values of KVLCC2 ship, which act depending on the variation of wave amplitudes at different wavelength, are shown in Figure 3. Since there are many studies for the KVLCC2 ship, the added resistance values obtained from mathematical model are compared with other results in the literature. It is obviously seen in Figure 3 that a ship has highest added resistance when the ratio λ/L_{pp} is nearly 1.0. When this ratio is considered as the peak, if this ratio increases or decreases, the added resistance value of ship decreases. However, if the ratio is less than approximately 0.5, the added resistance increases again.

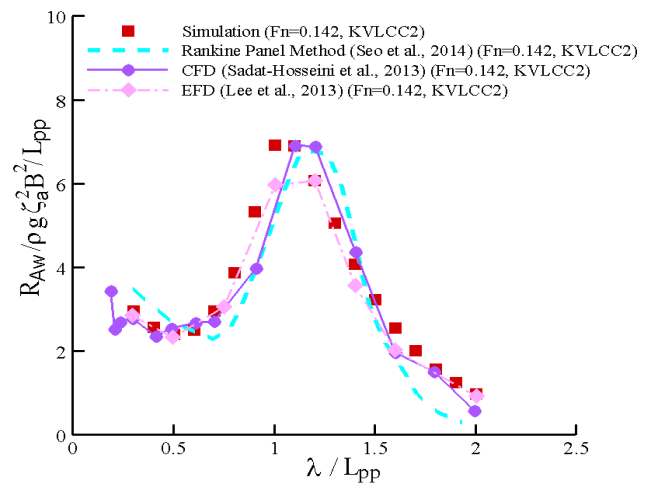


Figure 3. Added resistance for KVLCC2 ship

The values of Esso Osaka's added resistance for various wavelengths are obtained from the validated mathematical model. Figure 4 shows these obtained values in regular head waves. Just like the obtained added resistance values for KVLCC2, the orientations of the added resistance graphs in Figure 4 for the Esso Osaka ship are similar.

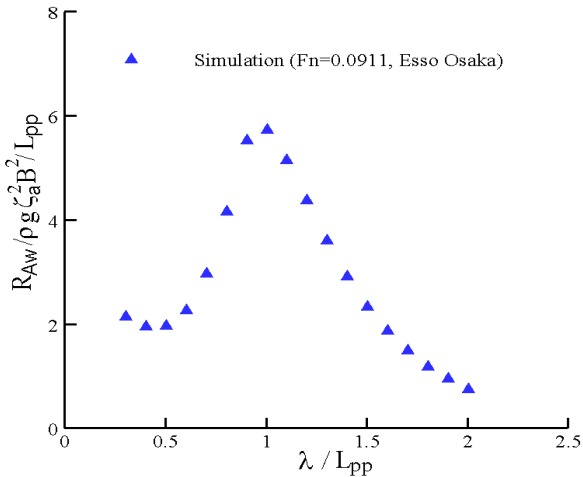


Figure 4. Added resistance for Esso Osaka ship

The Simulation of Turning Tests

The turning circle results for the Esso Osaka is obtained using the mathematical model. The turning circle simulation by assuming calm water are validated previous study (Budak, 2023) and the trial data are shown in Figure 5 for the Esso Osaka ship. Additionally, the turning tests given in Figure 5 are performed in regular head waves for Esso Osaka ship. In these simulations, the ratio (λ/L_{pp}) is equal to 1.0 and constant, however the values of the wave amplitudes are assumed as 0.5 m, 1.0 m, and 1.5 m. Although the ratio is equal to 1.0 in these simulations, as the wave amplitude increases, the added resistance of the ship increases, and the ship follows an elliptical rotation.

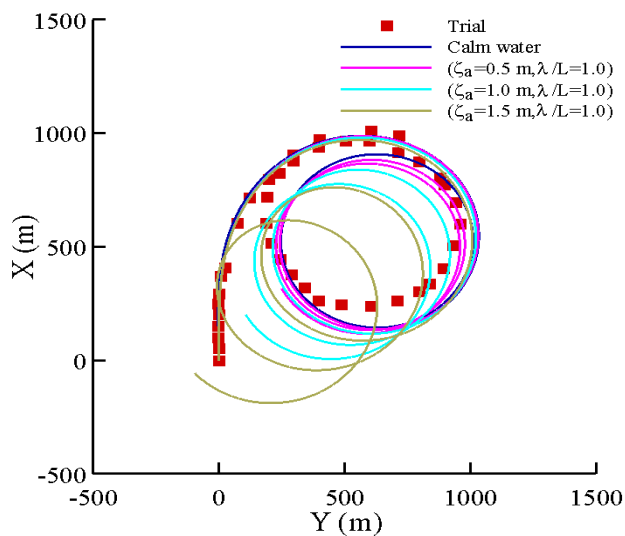


Figure 5. The comparison of obtained turning circle results

Simulation Cases

A course with fixed obstacles in some locations is determined for performing path following simulation. The ship velocity is assumed to be $U=5.144$ m/s. The mentioned mathematical model is used to obtain routes for two cases, calm water, and regular head waves. As the results of simulations, the ship can reach all randomly determined coordinates on the course for both cases. As shown in Figure 6, when the ship encounters an obstacle on her route, the ship modifies her route automatically to avoid the collisions and reaches the determined target destination safely. The oscillations in the fields of target coordinates shown in the Figure 6 are quite normal considering the obtained maneuvering characteristics of Esso Osaka ship. From this point of view, it can be understood that these oscillations in some fields where obstacles exist on the course are seen acceptable for Esso Osaka ship during the simulation. Moreover, the algorithm used to obtain a safe route achieves the purpose of this study as seen in Figure 6.

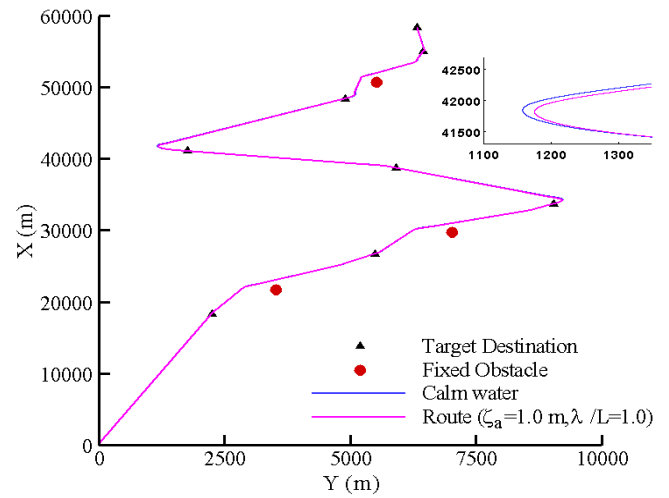


Figure 6. Path following simulations with avoidance collision

In the simulations, both different wavelengths and different wave amplitudes are considered. The path following simulation durations for determined course depend on the values of the wave amplitude and wavelength. However, in each simulation, it is concluded that the ship could reach the targeted destinations safely. Although more simulations with various wave amplitude and wavelength are performed using mathematical model, the path following simulations for regular head waves, determined as $\zeta_a=1.0$ m in wave amplitude and $\lambda/L_{pp}=1.0$ in ratio, and for calm water are shown in Figure 6 to show the differences clearly. However, the heading angle changings of Esso Osaka during the other simulations are

shown in Figure 7 to see the simulation times shown in Table 2. In all path following simulations, the angle of the regular waves acting on the initial ship position is 180°. However, it is emphasized that the acting angle of the regular waves to the ship changes since the ship maneuvers to reach the target coordinates, and the calculations are performed to calculate according to the changing angle of the wave in each time interval during the simulations. Various path following simulations are performed by changing the wavelength and amplitude values to determine the effects of the regular head waves.

the added resistance value at $\lambda/L_{pp} \sim 0.25$ has higher than at $\lambda/L_{pp} \sim 0.5$. For this reason, the simulation time at $\lambda/L_{pp} \sim 0.25$ is expected to be longer than the simulation time at $\lambda/L_{pp} \sim 0.5$. Moreover, since the ship needs to perform extra maneuvers to reach the target coordinates along the determined course, the simulation time increases. When the ratio $\lambda/L_{pp}=1.0$ and $\zeta_a=0.5$ are selected, the simulation time is 251.33 min. However, if the ratio $\lambda/L_{pp}=1.0$ and $\zeta_a=1.0$ are selected, the simulation time is 277.57 min. In another words, the simulation time for $\lambda/L_{pp}=1.0$ and $\zeta_a=0.5$ increases about 3.3% compared to the calm water while this increasing ratio is nearly 14% for $\lambda/L_{pp}=1.0$ and $\zeta_a=1.0$.

Table 2. The simulation times

$\frac{\lambda}{L}$	$\zeta_a = 0.5 \text{ m}$ Time (min.)	$\zeta_a = 1.0 \text{ m}$ Time (min.)
0.25	246.7	257.16
0.5	246.19	255.07
1.0	251.33	277.57
2.0	244.18	246.60
Calm water		243.40

Conclusion

A mathematical model including a maneuvering model and a control system is created within the scope of this article. The mathematical model is proposed to ensure that the ship can reach the desired coordinates by determining an automatic safe route. For this purpose, the maneuvering model and PD (Proportional Derivative) controller are combined to create the mathematical model. The added resistances for KVLCC2 ship are calculated in regular head waves with different wavelengths and compared to other studies in the literature for validation simulations. If the results are examined, while the highest value of added resistance for the KVLCC2 ship in regular head waves is when the wavelength to ship length ratio is nearly 1.0 ($\lambda/L_{pp} \sim 1.0$), the lowest value is when the ratio is nearly 2.0 ($\lambda/L_{pp} \sim 2.0$). The obtained added resistance results are compatible with the other studies in the literature. Similarly, the added resistance simulations are performed for Esso Osaka ship due to the chosen for path following simulations. Additionally, the turning tests are simulated for Esso Osaka in calm water, and regular head waves. Similarly, the path following simulations in regular head waves are performed not only in calm water but also in regular head waves with various wave amplitudes and wavelengths. In conclusion, considering the result of performed path following simulations, the time of simulation has been recorded as the longest when the ratio of λ/L_{pp} is ~ 1.0 . However,

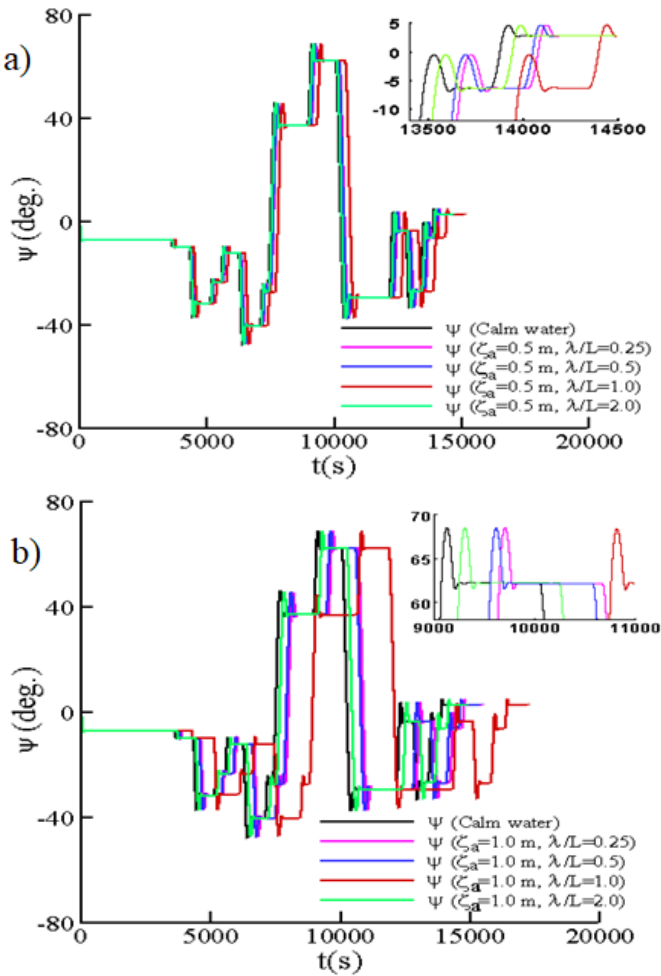


Figure 7. The heading angle for various wavelengths and amplitudes during the simulations, a) for $\zeta_a=0.5 \text{ m}$ and b) for $\zeta_a=1.0 \text{ m}$

The simulation times shown in Table 2 for path following simulations with various wavelengths and amplitudes. Considering the added resistance values obtained for the Esso Osaka ship in Figure 4, it is said that the highest added resistance occurs when the ratio nearly $\lambda/L_{pp}=1.0$. Therefore, in regular head waves with $\lambda \sim L_{pp}$, the added resistance value is higher for that ship, so ship velocity decreases even more than the others, and so the simulation time increases. In other words,

if λ/L_{pp} is the farther from the mentioned ratio ($\lambda/L_{pp} \sim 1.0$), the simulation time decreases until λ/L_{pp} is nearly 0.5. Moreover, in the case that λ/L_{pp} is less than ~ 0.5 , the simulation time commences to increase. As expected, the simulation time varies according to the added resistance value. When the added resistance value is high, the simulation time is longer, and when it is low, the simulation time is shorter. Furthermore, simulation results using mathematical model are shown that a ship in regular head waves may reach the target coordinates safely even if the ship encounters an obstacle on the determined course. In future studies, the other control systems named velocity controller, berthing controller, etc. can be added to the mathematical model to create an autonomous ship, thus the ship may be used more effectively for maritime transportation because of having an intelligent system.

Compliance With Ethical Standards

Conflict of Interest

The author declares that there is no conflict of interest.

Ethical Approval

For this type of study, formal consent is not required.

Data Availability Statement

All data generated or analyzed during this study are included in this published article.

References

- Abdel-latif, S., Abdel-geliel, M. & Zakzouk E. E. (2013). Simulation of ship maneuvering behavior based on the modular mathematical model. *International Conference on Aerospace Sciences and Aviation Technology, 15(Aerospace Sciences & Aviation Technology)*, Egypt, pp. 1-14. <https://doi.org/10.21608/asat.2013.22111>
- Akbar, A., Aasen, A., Msakni, M. K., Fagerholt, K., Lindstad, E. & Meisel, F. (2021). An economic analysis of introducing autonomous ships in a short-sea liner shipping network. *International Transactions in Operational Research*, 28(4), 1740-1764. <https://doi.org/10.1111/itor.12788>
- Aksu, E., & Köse, E. (2017). Evaluation of mathematical models for tankers' maneuvering motions. *Journal of ETA Maritime Science*, 5(1), 95-109. <https://dx.doi.org/10.5505/jems.2017.52523>
- Beji, S. (2020). Formulation of wave and current forces acting on a body and resistance of ships. *Ocean Engineering*, 218, 108121. <https://doi.org/10.1016/j.oceaneng.2020.108121>
- Budak, G. (2023). The effect of controller selection in collision avoidance system on fuel consumption for unmanned surface vessel: a case study. *Ships and Offshore Structures*, 18(2), 315-323. <https://doi.org/10.1080/17445302.2022.2157131>
- Çakıcı, F., Kahramanoglu, E., & Alkan, A. D. (2017). Numerical prediction of vertical ship motions and added resistance. *Transactions of the Royal Institution of Naval Architects Part A: International Journal of Maritime Engineering*, 159(Part A4), 393-402. <https://doi.org/10.3940/rina.ijme.2017.a4.450>
- Chen, Y. Y., Ellis-Tiew, M. Z., Chen, W. C., & Wang, C. Z. (2021). Fuzzy risk evaluation and collision avoidance control of unmanned surface vessels. *Applied Sciences*, 11(14), 6338. <https://doi.org/10.3390/app11146338>
- Degre, T., & Lefevre, X. (1981). A collision avoidance system. *Journal of Navigation*, 34(2), 294-302. <https://doi.org/10.1017/S0373463300021408>
- Fang, M. -C., Luo, J. -H., & Lee, M. -L. (2005). A nonlinear mathematical model for ship turning circle simulation in waves. *Journal of Ship Research*, 49(2), 69-79. <https://doi.org/10.5957/jsr.2005.49.2.69>
- Fossen, T. (2002). *Marine Control Systems: Guidance, Navigation and Control of Ships, Rigs and Underwater Vehicles*. Marine Cybernetics.
- He, Y., Li, Z., Mou, J., Hu, W., Li, L., & Wang, B. (2021). Collision-avoidance path planning for multi-ship encounters considering ship manoeuvrability and COLREGs. *Transportation Safety and Environment*, 3(2), 1-11. <https://doi.org/10.1093/tse/tdab004>
- Hirdaris, S., Bai, W., Dessi, D., Ergin, A., Gu, X., Hermundstad, O., Huijsmans, R., Iijima, K., Nielsen, U., Parunov, J., Fonseca, N., Papanikolaou, A., Argyriadis, K., & Incecik, A. (2014). Loads for use in the design of ships and offshore structures. *Ocean Engineering*, 78, 131-174. <https://doi.org/10.1016/j.oceaneng.2013.09.012>
- Jin, Y., Yiew, L., Zheng, Y., Magee, A., Duffy, J., & Chai, S. (2021). Dynamic manoeuvres of KCS with CFD free-running computation and system-based modelling. *Ocean Engineering*, 241, 110043. <https://doi.org/10.1016/j.oceaneng.2021.110043>

- Kafali, M., & Aksu, E. (2022). A multi-objective optimization model for determining the performance of a sailboat. *Journal of ETA Maritime Science*, 10(3), 177-184. <https://doi.org/10.4274/jems.2022.24392>
- Kobayashi, H., Blok, J., Barr, R., Kim, Y. S., & Nowicki, J. (2002). Specialist committee on Esso Osaka: Final report and recommendations to the 23rd ITTC. *23rd International Towing Tank Conference*, pp. 8-14.
- Kurt, I., & Aymelek, M. (2022). Operational and economic advantages of autonomous ships and their perceived impacts on port operations. *Maritime Economics & Logistics* 24(2), 302-326. <https://doi.org/10.1057/s41278-022-00213-1>
- Lang, X., & Mao, W. (2020). A semi-empirical model for ship speed loss prediction at head sea and its validation by full-scale measurements. *Ocean Engineering*, 209, 107494. <https://doi.org/10.1016/j.oceaneng.2020.107494>
- Lee, J. H., Seo, M. G., Park, D. M., Yang, K. K., Kim, K. H., & Kim, Y. (2013). Study on the effects of hull form on added resistance. *Proceedings of the 12th International Symposium on Practical Design of Ships and Other Floating Structures*. Korea, pp. 329-337.
- Li, G., & Zhang, X. (2022). Research on the influence of wind, waves, and tidal current on ship turning ability based on Norrbinn Model. *Ocean Engineering*, 259, 111875. <https://doi.org/10.1016/j.oceaneng.2022.111875>
- Liu, L., Zhang, L., Zhang, S., & Cao, S. (2020) Multi-UUV cooperative dynamic maneuver decision-making algorithm using intuitionistic fuzzy game theory. *Complexity*, 2020, 2815258. <https://doi.org/10.1155/2020/2815258>
- Liu, S., & Papanikolaou, A. (2016). Fast approach to the estimation of the added resistance of ships in head waves. *Ocean Engineering*, 112, 211-225. <https://doi.org/10.1016/j.oceaneng.2015.12.022>
- Liu, S., & Papanikolaou, A. (2017). Approximation of the added resistance of ships with small draft or in ballast condition by empirical formula. *Proceedings of the IMechE Part M: Journal of Engineering for the Maritime Environment*, 223(1), 27-40. <https://doi.org/10.1177/1475090217710099>
- Lyu, H. G., & Yin, Y. (2017). Ship's trajectory planning for collision avoidance at sea based on modified artificial potential field. *2nd International Conference on Robotics and Automation Engineering*, (Icrae) Shanghai, pp. 351-357.
- Mohamed-Seghir, M., Kula, K., & Kouzou, A. (2021). Artificial intelligence-based methods for decision support to avoid collisions at sea. *Electronics*, 19(10), 2360. <https://doi.org/10.3390/electronics10192360>
- Moreira, L., Fossen, T. I., & Soares, C. G. (2007) Path following control system for a tanker ship model. *Ocean Engineering*, 34, (14,15), 2074-2085. <https://doi.org/10.1016/j.oceaneng.2007.02.005>
- Ogawa, A., & Kasai, H. (1978). On the mathematical model of maneuvering motion of ships. *International Shipbuild Progress*, 25, 306-319.
- Ozdemir, Y., & Barlas, B. (2017). Numerical study of ship motions and added resistance in regular incident waves of KVLCC2 model. *International Journal of Naval Architecture and Ocean Engineering*, 9, 149-159. <https://doi.org/10.1016/j.ijnaoe.2016.09.001>
- Park, D. -M. Kim, Y., Seo, M. -G., & Lee, J. (2016). Study on added resistance of a tanker in head waves at different drafts. *Ocean Engineering*, 111, 569-581. <https://doi.org/10.1016/j.oceaneng.2015.11.026>
- Perera, L. P., Carvalho, J. P., & Soares, C. G. (2010). Bayesian network based sequential collision avoidance action execution for an ocean navigational system. *IFAC Proceedings*, 43(20), 266-271.
- Praczyk, T. (2015). Neural anti-collision system for autonomous surface vehicle. *Neurocomputing*, 149, 559-572. <https://doi.org/10.1016/j.neucom.2014.08.018>
- Sadat-Hosseini, H., Wu, P., Carrica, P., Kim, H., Toda, Y., & Stern, F. (2013). CFD verification and validation of added resistance and motions of KVLCC2 with fixed and free surge in short and long head waves. *Ocean Engineering*, 59, 240-273. <https://doi.org/10.1016/j.oceaneng.2012.12.016>
- Suo, Y., Chen, W., Claramunt, C., & Yang, S. (2020). A ship trajectory prediction framework based on a recurrent neural network. *Sensors*, 20, 5133. <https://doi.org/10.3390/s20185133>

- Szelangiewicz, T., Wiśniewski, B., & Żelazny, K. (2014). The influence of wind, wave and loading condition on total resistance and speed of the vessel. *Polish Maritime Research*, 21(3), 61-67. <https://doi.org/10.2478/pomr-2014-0031>
- Tsou, M. C., & Hsueh, C. K. (2010). The study of ship collision avoidance route planning by ant colony algorithm. *Journal of Marine Science and Technology*, 18(5), 746-756. <https://doi.org/10.51400/2709-6998.1929>
- Tsujimoto, M., Shibata, K., & Kuroda, M. (2008). A practical correction method for added resistance in waves. *Journal of the Japan Society of Naval Architects and Ocean Engineers*, 8, 177-184. <https://doi.org/10.2534/jjasnaoe.8.177>
- Wang, C., & Fu, Y. (2020). Ship trajectory prediction based on attention in bidirectional recurrent neural networks. *5th International Conference on Information Science, Computer Technology and Transportation (ISCTT)*, Shenyang, China, pp. 529–533.
- Xie, Z., Falzarano, J. M., & Wang, H. (2020). A framework of numerically evaluating a maneuvering vessel in waves. *Journal of Marine Science and Engineering*, 8(6), 392. <https://doi.org/10.3390/jmse8060392>
- Yasukawa, H., & Sakuno, R. (2019). Application of the mmg method for the prediction of steady sailing condition and course stability of a ship under external disturbances. *Journal of Marine Science and Technology*, 25, 196–220. <https://doi.org/10.1007/s00773-019-00641-4>
- Yasukawa, H., & Yoshimura, Y. (2015). Introduction of mmg standard method for ship maneuvering predictions. *Journal of Marine Science and Technology*, 20, 37–52. <https://doi.org/10.1007/s00773-014-0293-y>
- Zaccone, R., & Martelli, M. (2020). A collision avoidance algorithm for ship guidance applications. *Journal of Marine Engineering & Technology*, 19, 62-75. <https://doi.org/10.1080/20464177.2019.1685836>
- Zhao, W., Wang, Y., Zhang, Z., & Wang, H. (2021). Multicriteria ship route planning method based on improved particle swarm optimization–genetic algorithm. *Journal of Marine Science and Engineering*, 9(4), 357. <https://doi.org/10.3390/jmse9040357>
- Zhou, Z., Zhang, Y., & Wang, S. A. (2021). Coordination system between decision making and controlling for autonomous collision avoidance of large intelligent ships. *Journal of Marine Science and Engineering*, 9(11), 1202. <https://doi.org/10.3390/jmse9111202>